

A parametrization of the effects of cloud and precipitation overlap for use in general-circulation models

By CHRISTIAN JAKOB^{1*} and STEPHEN A. KLEIN²

¹*European Centre for Medium-Range Weather Forecasts, UK*

²*Geophysical Fluid Dynamics Laboratory/NOAA, USA*

(Received 13 September 1999; revised 9 February 2000)

SUMMARY

The necessity for treating the effects of vertically varying cloud fraction when parametrizing microphysical processes in general-circulation models (GCMs) was recently highlighted by Jakob and Klein. In this study a parametrization to include such effects in a GCM is developed, and the new scheme is applied in the ECMWF global model. The basic idea of the new scheme is to separate the model's rain and snow fluxes into a cloudy and a clear-sky part. The scheme is tested using the subgrid-scale precipitation model of Jakob and Klein as a benchmark. The impact of the new scheme on the model climate is also investigated.

It is shown that the new parametrization leads to a better representation of the effects of cloud and precipitation overlap, and that it alleviates most of the problems connected with their treatment in the current scheme. Due to the better treatment of cloud and precipitation overlap the new parametrization leads to a reduction in precipitation evaporation and an increase in accretion rates. When tested in seasonal model integrations the new scheme produces a drier tropical mid-troposphere with consequences for the hydrological cycle.

KEYWORDS: Cloud parametrization General-circulation model Precipitation

1. INTRODUCTION

Cloud parametrizations in general-circulation models (GCMs) have changed their character over the last few years. Almost all GCMs already use, or plan to use, at least one prognostic equation for cloud condensate. This development necessitates an increased sophistication in the description of microphysical processes. In diagnostic descriptions of clouds (e.g. Manabe *et al.* 1965) the generation of precipitation was simply achieved by precipitating out all condensate formed when removing supersaturation at the grid-scale. The desire to 'leave some condensate behind' as cloud demands at least a simple description of the manifold conversion processes from cloud to precipitation size particles, normally referred to as cloud microphysics. Many attempts to improve the description of these processes in GCMs have been reported on in the recent literature (e.g. Ghan and Easter 1992; Bechthold *et al.* 1993; Fowler *et al.* 1996; Lohmann and Roeckner 1996; Rotstajn 1997).

One inherent difficulty in the description of cloud microphysics is that the processes take place on scales that are significantly smaller than GCM grid-boxes. For many of the processes it is the local environment that determines parameters such as evaporation rates etc. An additional complication arises from the fact that most GCMs predict the occurrence of clouds over only part of their grid-box using a cloud-fraction parametrization of some form (e.g. Slingo 1987; Sundqvist 1988; Smith 1990; Tiedtke 1993; Rasch and Kristjansson 1998). This introduces problems in even knowing which part of the microphysical parametrizations to employ. If the precipitation produced by the stratiform cloud is falling inside the cloud, then a collection/aggregation parametrization should be applied. If the precipitation is falling outside the cloud, then the evaporation-of-precipitation part of the parametrization scheme needs to be used.

Only little attention has been paid to the effects of cloud overlap on the parametrization of precipitation so far. The first to consider such effects by adjusting microphysical parameters, such as autoconversion and accretion rates in case of vertically varying

* Corresponding author: ECMWF, Shinfield Park, Reading, Berkshire RG2 9AX, UK.

cloud, were Bechthold *et al.* (1993). Rotstayn (1997) introduced a precipitation fraction into his cloud parametrization to capture some of the overlap effects. In a recent study, Jakob and Klein (1999, hereafter JK99) attempted to evaluate the importance of the 'cloud macrophysics', i.e. the treatment of cloud cover and its vertical overlap, for the parametrization of microphysical processes. They used the simple microphysical scheme of Sundqvist (1988) as implemented in the current European Centre for Medium-Range Weather Forecasts (ECMWF) model (Tiedtke 1993, hereafter T93) to show that a more detailed treatment of cloud fraction and overlap can lead to large differences in the parametrized precipitation and evaporation rates. These differences are especially large in the tropics, where large vertical variations in cloud cover exist in the ECMWF model. The method they employed was to divide each model grid-box into a number of smaller boxes which, after applying the model's cloud-overlap assumption, are assumed to be either cloudy or cloudless. They then solved the cloud microphysics parametrization for each of the boxes individually and averaged the results to yield grid-mean precipitation and heating/moistening rates.

Applying this method in the ECMWF model increased the overall model computational cost by 15 to 20%. It is very likely that if a more sophisticated microphysical parametrization were used the increase in cost would be even larger. Given the large computational cost together with existing uncertainties in both the microphysical parametrizations themselves and in the description of the cloud overlap it seems inappropriate to apply the JK99 'subgrid precipitation scheme' directly in a GCM. However, it can also be argued that the use of a complex microphysical parametrization, which undoubtedly also increases model cost enormously, is less useful before the two major problem areas identified in JK99, namely the need for a description of the area of the grid-box covered with precipitation and an independent treatment of precipitation inside and outside cloud, are addressed. The first of these issues has been considered in some previous studies (e.g. Rotstayn 1997), whereas to the authors' knowledge no parametrization addressing the latter exists in a GCM.

The present paper describes a simple parametrization that tries to address both points. The basic idea is to divide the precipitation flux in each grid-box into a cloudy and a clear-sky part, and to describe the area coverage of each of the flux components and their overlap. Within the limits of current cloud-overlap assumptions this approach solves the first-order problem of which part of the microphysical scheme to apply over which part of the grid-box. It will be shown that the new parametrization captures most of the main features of the subgrid precipitation formulation of JK99 at a much reduced cost.

In section 2, after a short description of the current parametrization, the new parametrization is introduced. Section 3 contains comparisons of results of the new parametrization to both the current, and to JK99's sub-grid precipitation scheme, in order to demonstrate the ability of the new scheme to address the main problems raised in JK99. Section 4 contains a description of the impact of the new scheme on the model climate. This is followed by a discussion in section 5, with conclusions presented in section 6.

2. DESCRIPTION OF THE STRATIFORM PRECIPITATION PARAMETRIZATION

Within large-scale models, stratiform precipitation is usually treated diagnostically such that the vertical divergence of the downward flux of precipitation is balanced by the microphysical sources (e.g. precipitation formation) and sinks (e.g. precipitation

evaporation) (e.g. Heymsfield and Donner 1990; Ghan and Easter 1992):

$$g \frac{\partial}{\partial p} (\rho l_P V_P) = S_P, \quad (1)$$

where g is gravitational acceleration, p is pressure, ρ is density, l_P is the specific humidity of precipitation condensate, V_P is the mass-weighted fall speed of the precipitation mass, and S_P is the time rate of change of precipitation mass due to microphysical sources and sinks, with units of kg condensate (kg air)⁻¹s⁻¹. Equation (1) ignores the time tendency of precipitation condensate which is reasonable given that the time for precipitation to reach the surface is often considerably less than the time step of the parametrized microphysics. From this equation, the downward flux of precipitation mass P , at a given pressure p , is the vertical integral of the sources and sinks of precipitation at all higher levels:

$$P(p) \equiv \rho l_P V_P = \frac{1}{g} \int_0^p S_P dp'. \quad (2)$$

(a) *Original parametrization*

T93 represented the downward precipitation flux by a single mean value for the grid-cell,

$$\bar{P} \equiv \frac{1}{A} \int P dA, \quad (3)$$

where A is the area covered by the grid-cell. The fractional area of the grid-cell in which the precipitation rate is greater than zero is denoted

$$a_P \equiv \frac{1}{A} \int H(P) dA, \quad (4)$$

where $H(x)$ is a unit step function defined as equal to 1 if $x > 0$, and zero otherwise. Within the area a_P , the parametrization implicitly assumes that the local value of the precipitation rate P is uniformly equal to \bar{P}/a_P .

The fractional area covered by precipitation at the bottom of a model level, k , is given by:

$$a_{P,k} = \max \left(a_{P,k-1}, \frac{a_k \Delta \bar{P}_k + a_{P,k-1} \bar{P}_{k-1}}{\Delta \bar{P}_k + \bar{P}_{k-1}} \right), \quad (5)$$

where

$$\Delta \bar{P}_k \equiv \frac{1}{A} \int \left(\frac{1}{g} \int_{p_t}^{p_b} S_P \cdot H(S_P) dp' \right) dA \quad (6)$$

is the increase in \bar{P} due to the microphysical sources of precipitation (e.g. autoconversion, accretion, ice-settling, etc.) from the pressure at the top of the grid-cell, p_t , to the pressure at the base of the grid cell, p_b . The index of the model levels, k , is assumed to increase downwards. The second option of the maximum operator in (5) is a weighted average of the cloud fraction of level k , a_k , and the precipitation area at the top of the grid-cell, $a_{P,k-1}$, where the weights are the fraction of the precipitation at the base of level k that originated from level k and the fraction of the precipitation at the base of

level k that originated from higher levels, respectively. By weighting the precipitation source by a_k , T93 implicitly assumes that the whole area of the cloud contributes to the precipitation source. Note that T93 assumes that clouds fill the vertical extent of a grid-cell completely such that the fraction of the volume which contains clouds is equal to the fraction of the area which contains clouds. The maximum operator prevents $a_{P,k}$ from decreasing when (5) is solved from the model top to the surface. Only in the case that all of the precipitation evaporates in a given level does $a_{P,k}$ return to zero. In determining precipitation evaporation, the fractional area in which precipitation is evaporating is assumed to be $\max(0, a_{P,k} - a_k)$. This assumes a maximum overlap between the area containing stratiform precipitation and the cloudy area. The local value of the precipitation rate in the area where precipitation is evaporating is assumed to be $(\Delta \bar{P}_k + \bar{P}_{k-1})/a_{P,k}$. Note that precipitation generated in level k may evaporate in the same level if $a_{P,k-1} > a_k$; this is inconsistent with the assumption that, where it occurs, cloudy air completely fills the vertical extent of the grid-cell.

(b) *New parametrization*

The main difference between the new and old parametrization is that in the new scheme the precipitation flux is represented by mean values for the cloudy and clear portions of the grid-cell (see Fig. 1). That is, the grid-cell mean precipitation flux in cloudy areas is defined by:

$$P^{\text{cld}} \equiv \frac{1}{A} \int P \cdot H(l) \, dA, \quad (7)$$

where the step function marks the portion of the grid-cell containing cloud with a condensate specific humidity l . The fractional area which contains the cloudy precipitation flux is denoted by

$$a_P^{\text{cld}} \equiv \frac{1}{A} \int H(l)H(P) \, dA. \quad (8)$$

Within the area containing the cloudy precipitation flux, the local precipitation rate P is assumed to be uniform with the value $P^{\text{cld}}/a_P^{\text{cld}}$. Similarly the grid-cell mean precipitation flux in clear areas and the fractional area containing precipitation flux in clear areas are:

$$P^{\text{clr}} \equiv \frac{1}{A} \int P \cdot (1 - H(l)) \, dA, \quad (9)$$

and

$$a_P^{\text{clr}} \equiv \frac{1}{A} \int (1 - H(l))H(P) \, dA, \quad (10)$$

respectively. Within the area containing the clear precipitation flux, P is assumed to be uniform with the value $P^{\text{clr}}/a_P^{\text{clr}}$. With these definitions, $\bar{P} = P^{\text{cld}} + P^{\text{clr}}$ and $a_P = a_P^{\text{cld}} + a_P^{\text{clr}}$.

The method to determine a_P^{cld} and a_P^{clr} is as follows. If precipitation is generated in a particular level through the processes of autoconversion or ice sedimentation, it is assumed to be generated in the cloud uniformly and thus at the base of level k , $a_{P,k}^{\text{cld}} = a_k$. The precipitation generated in this cloudy region is given by:

$$\Delta P_k^{\text{cld}} \equiv \frac{1}{A} \int \left(\frac{1}{g} \int_{p_t}^{p_b} S_P \cdot H(l) \, dp' \right) \, dA, \quad (11)$$

and the cloudy precipitation flux at the base of level k is given by $P_k^{\text{cld}} = \tilde{P}_k^{\text{cld}} + \Delta P_k^{\text{cld}}$, where the tilde symbol indicates the value of P^{cld} at the top of level k . Because the cloud is assumed to be internally homogeneous, (11) simplifies to

$$\Delta P_k^{\text{cld}} = a_k S_P^{\text{cld}} \frac{(p_b - p_t)}{g}, \quad (12)$$

where S_P^{cld} is the generation rate of precipitation inside the cloud. If only accretion occurs in the clouds of level k , $a_{P,k}^{\text{cld}}$ equals $\tilde{a}_{P,k}^{\text{cld}}$, the fractional area that contains cloudy precipitation flux at the top of level k .

Because the clear precipitation flux is assumed to be horizontally uniform, evaporation does not alter the area containing clear precipitation flux such that $a_{P,k}^{\text{clr}} = \tilde{a}_{P,k}^{\text{clr}}$. Only in the case that all of the clear precipitation flux evaporates in level k does $a_{P,k}^{\text{clr}} = 0$. The clear-sky precipitation flux at the base of level k is given by $P_k^{\text{clr}} = \tilde{P}_k^{\text{clr}} + \Delta P_k^{\text{clr}}$, where \tilde{P}_k^{clr} is the clear-sky precipitation flux at the top of level k , and

$$\Delta P_k^{\text{clr}} = \frac{1}{A} \int \left(\frac{1}{g} \int_{p_t}^{p_b} S_P \cdot (1 - H(l)) dp' \right) dA = \tilde{a}_{P,k} S_P^{\text{clr}} \frac{(p_b - p_t)}{g}, \quad (13)$$

where $S_P < 0$ indicates precipitation evaporation. Note that, in the new parametrization, precipitation evaporation is a function of \tilde{P}_k^{clr} guaranteeing that precipitation generated in a level cannot evaporate in the same level. This will ensure consistency with the assumption that clouds where present fill the vertical extent of the grid cell, and that horizontal transfer of precipitation mass from cloudy to clear regions of the grid cell is not possible.

At the interfaces between levels, precipitation mass that is in cloud at the upper level may fall into clear air of the lower level, or precipitation mass that is in clear air of the upper level may fall into cloud of the lower level. Thus at level interfaces an algorithm is needed to transfer precipitation and its area between the cloudy and clear portions of the grid-box. The algorithm is constructed by determining the amount of area associated with each transfer and then transferring precipitation fluxes between clear and cloudy components according to the assumption that the precipitation flux is horizontally uniform but with different values in the clear and cloudy regions containing precipitation.

At level interfaces, there are four possible areas to be defined (Fig. 1): the area in which cloudy precipitation flux falls into cloud of the lower level, the area in which cloudy precipitation flux falls into clear air of the lower level, the area in which clear precipitation flux falls into clear air of the lower level, and the area in which clear precipitation flux falls into cloud of the lower level. To determine these areas, the cloud-overlap assumption is applied to determine the relative horizontal location of clouds in the upper and lower levels. For the ECMWF model, the cloud-overlap assumption is expressed in terms of an equation which relates the total horizontal area C covered by clouds in levels 1 to k (where $k = 1$ is the top level of the model), to the total horizontal area covered by clouds in levels 1 to $k - 1$:

$$(1 - C_k) = (1 - C_{k-1}) \cdot \frac{1 - \max(a_k, a_{k-1})}{1 - \min(a_{k-1}, 1 - \delta)}, \quad (14)$$

where δ is set to 10^{-6} to prevent division by zero. Equation (14) gives maximum overlap for clouds in adjacent levels with cloud fraction monotonically increasing or decreasing with height, and random overlap for clouds either separated by clear levels or for levels

of changing sign in the vertical gradient of cloud fraction. From this equation, one can determine the portion of clouds of the lower level that is not overlapped by clouds at all higher levels; this area, $\Delta C = C_k - C_{k-1}$, cannot have any precipitation falling into it. Using this assumption, the area for which cloudy precipitation flux falls into clear air of the level below is given by

$$\Delta a_{P, \text{cld} \rightarrow \text{clr}} = a_{P, k-1}^{\text{cld}} - \min(a_k - \Delta C, a_{P, k-1}^{\text{cld}}). \quad (15)$$

Equation (15) makes the further assumption that there is maximum overlap between the area covered by cloudy precipitation at the base of the upper level and the portion of the lower-level cloud which lies beneath clouds in higher levels, $a_k - \Delta C$. With the assumption that the precipitation flux is horizontally uniform, the amount of cloudy precipitation flux of the upper level that falls into clear air of the level below is

$$\Delta P_{\text{cld} \rightarrow \text{clr}} = \frac{\Delta a_{P, \text{cld} \rightarrow \text{clr}}}{a_{P, k-1}^{\text{cld}}} \cdot P_{k-1}^{\text{cld}}. \quad (16)$$

The area in which clear precipitation flux of the upper level falls into cloud of the level below is

$$\Delta a_{P, \text{clr} \rightarrow \text{cld}} = \max\{0, \min(a_{P, k-1}^{\text{clr}}, a_k - \Delta C - a_{k-1})\}, \quad (17)$$

which assumes maximum overlap between the portion of the cloud in the lower level k which has cloud above it at some higher level other than $k - 1$, and the area covered by the clear precipitation flux. Again, with the assumption that the precipitation flux is horizontally uniform, the amount of clear precipitation flux of the upper level that falls into cloud of the level below is

$$\Delta P_{\text{clr} \rightarrow \text{cld}} = \frac{\Delta a_{P, \text{clr} \rightarrow \text{cld}}}{a_{P, k-1}^{\text{clr}}} \cdot P_{k-1}^{\text{clr}}. \quad (18)$$

Finally, the areas and fluxes at the top of level k can be related to those at the base of level $k - 1$ by

$$\tilde{a}_{P, k}^{\text{cld}} = a_{P, k-1}^{\text{cld}} + \Delta a_{P, \text{clr} \rightarrow \text{cld}} - \Delta a_{P, \text{cld} \rightarrow \text{clr}}, \quad (19)$$

$$\tilde{a}_{P, k}^{\text{clr}} = a_{P, k-1}^{\text{clr}} - \Delta a_{P, \text{clr} \rightarrow \text{cld}} + \Delta a_{P, \text{cld} \rightarrow \text{clr}}, \quad (20)$$

$$\tilde{P}_k^{\text{cld}} = P_{k-1}^{\text{cld}} + \Delta P_{\text{clr} \rightarrow \text{cld}} - \Delta P_{\text{cld} \rightarrow \text{clr}}, \quad (21)$$

$$\tilde{P}_k^{\text{clr}} = P_{k-1}^{\text{clr}} - \Delta P_{\text{clr} \rightarrow \text{cld}} + \Delta P_{\text{cld} \rightarrow \text{clr}}. \quad (22)$$

From these equations it is clear that the total precipitation area, $a_{P, k-1}^{\text{cld}} + a_{P, k-1}^{\text{clr}}$, and the precipitation flux, $P_{k-1}^{\text{cld}} + P_{k-1}^{\text{clr}}$, are conserved at level interfaces.

Figure 1 shows a schematic of the new scheme with some examples of the areas and transitions outlined above. Shown are four model layers with the grey areas indicating clouds. The arrows represent the precipitation fluxes in clouds (P_{cld}) and clear sky (P_{clr}). The width of the arrows indicates the magnitude of the flux. All precipitation starts as cloudy in the top layer. Part of it is then converted into clear-sky precipitation when falling into the next layer. The precipitation in cloud is enhanced whereas the clear-sky part is reduced by evaporation. Three distinct areas exist at the interface between the second and third layer. A cloud-to-cloud transition, a clear-sky-to-cloud transition and a clear-sky-to-clear-sky transition. Since the precipitation in the cloudy part of the third layer originates partly in cloudy sky and partly in clear sky above, an implied

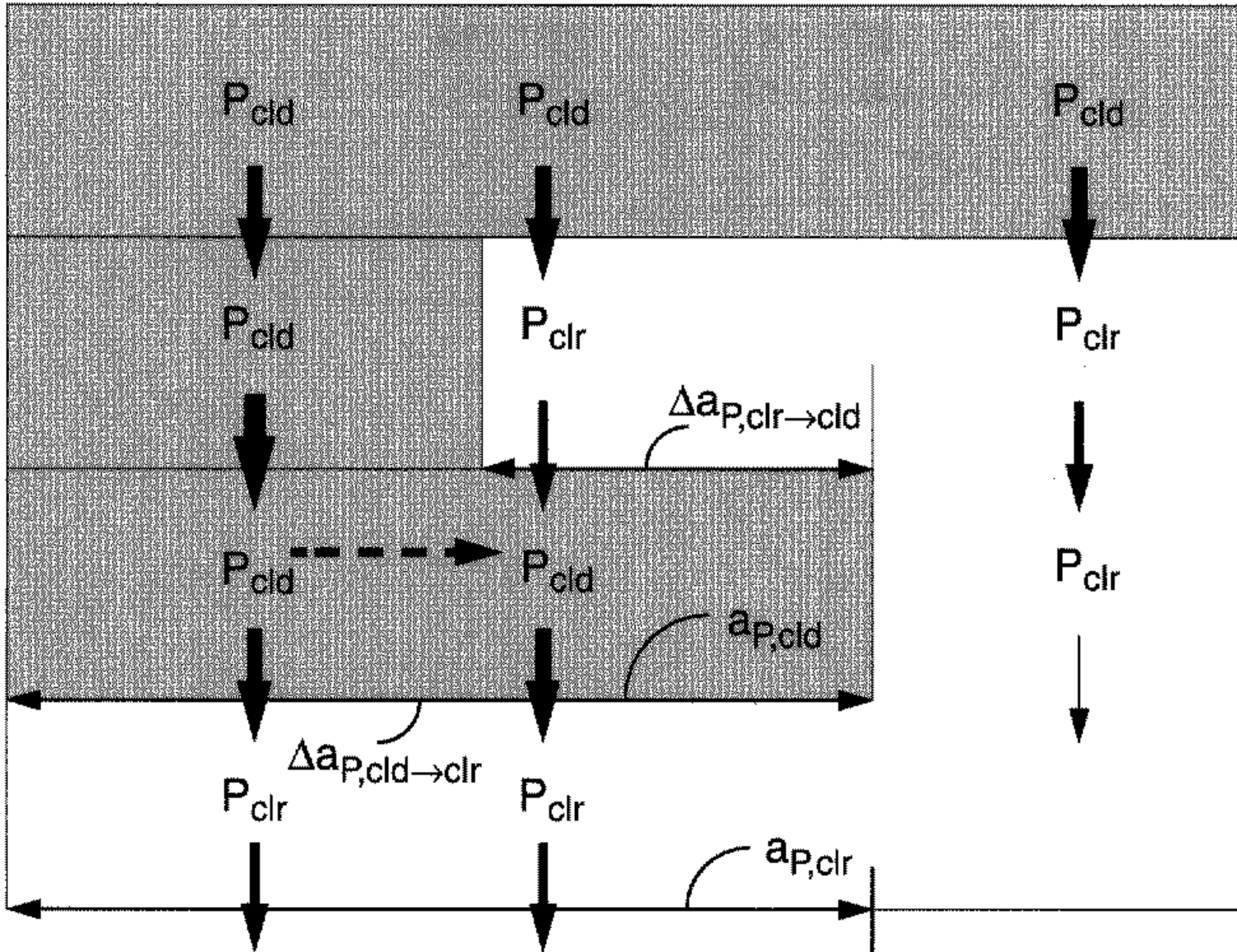


Figure 1. Schematic of the new parametrization scheme. For a detailed explanation see text.

horizontal flux (indicated by the dashed arrow) exists due to the averaging of the two incoming contributions into one cloudy flux. This is one of the remaining shortcomings of the new scheme whose effect will be outlined in the next section. In the part of the grid-box that is clear sky in all levels below the first, evaporation leads to the complete removal of precipitation when reaching the bottom of the lowest level, so that clear-sky precipitation only exists underneath the part of the grid-box that has cloud in more than one layer. With this concept in mind, the next section evaluates the new parametrization using the JK99 subgrid precipitation model as a reference.

3. COMPARISON OF THE NEW PARAMETRIZATION WITH THE JK99 SUBGRID MODEL

The two main reasons for developing the new parametrization were (i) the failure of the current parametrization to predict the correct area coverage of precipitation, and (ii) the inadequacy of the use of a single flux of precipitation to describe the microphysically different regimes inside and outside clouds. Both lead to an overestimation of evaporation of precipitation when compared with the JK99 subgrid precipitation model. The results given by this model might be far from the truth as measured by observations due to inadequacies in the prediction of the cloud fields and in the actual microphysical formulations. However, the JK99 model was designed and used only to examine the effects of vertical cloud-fraction variations on precipitation microphysics for a fixed set of cloud and microphysical parametrizations. In that context it does represent the truth for a parametrization attempting to capture those effects. It is, therefore, a valid test to compare the behaviour of the new parametrization described above against this model which resolves the horizontal rates and area covered by stratiform precipitation.

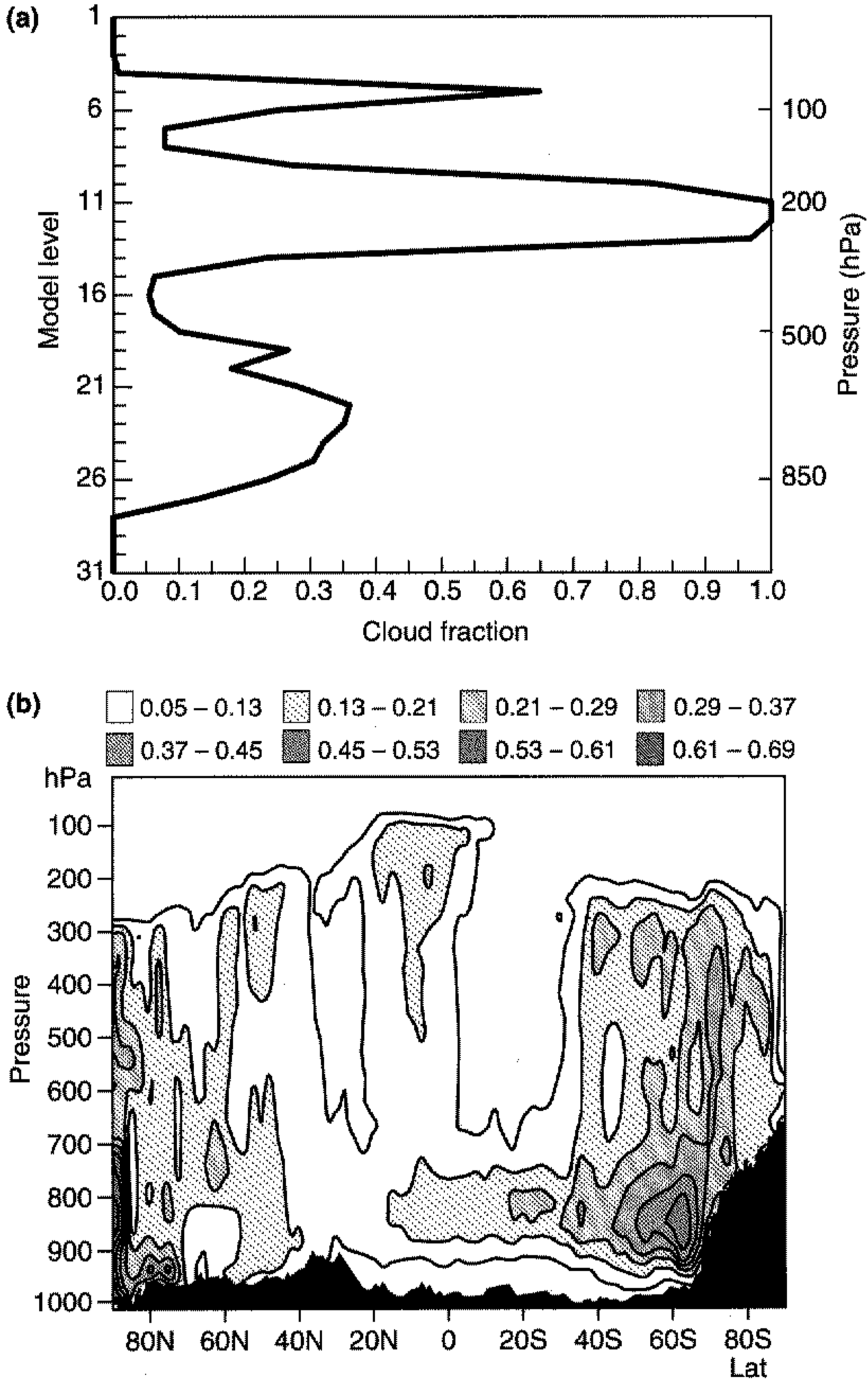


Figure 2. Initial cloud-fraction distribution for the single time-step experiments for (a) the single-column model and (b) the global model.

In this section the results of the current and the new parametrization of cloud and precipitation overlap will be compared against the subgrid model of JK99. The approach taken in JK99 to concentrate on single time-step experiments performed with both the single-column version and the full ECMWF model will be followed. This way feedback processes cannot occur, and the results indicate the direct physical effect of the parametrizations. The initial conditions used for the experiments are identical to those of JK99 and are shown for cloud fraction in Fig. 2.

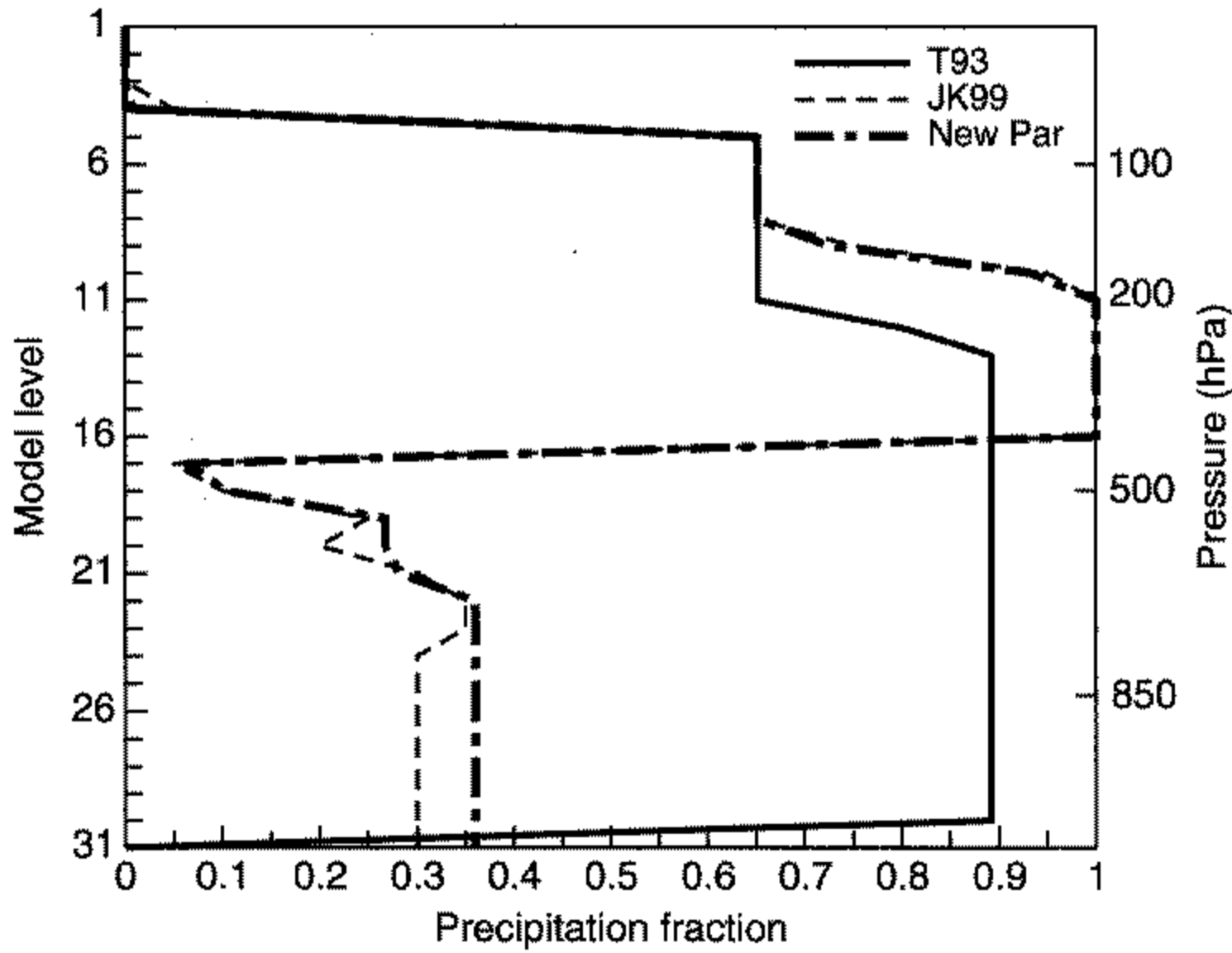


Figure 3. Precipitation fraction at a single tropical point as predicted in a single time step by the T93 parametrization, the JK99 subgrid model, and the new parametrization (New Par). See text for further explanation.

(a) *Single-column model*

Figure 3 shows the fractional area of a grid-box that is covered with precipitation as predicted by the JK99 subgrid model, by the T93 parametrization, and by the new parametrization. It is evident that the new parametrization yields results that are very close to the subgrid model. In fact from model level 1 to 20 the differences are entirely due to the rounding applied in the JK99 model which assumes cloud cover to change in steps of 0.05. The discrepancies below that level are still very small but are the result of the new formulation and will be discussed below.

As shown by JK99, the correct prediction of the precipitation fraction is a necessary but not sufficient condition to account for cloud-overlap effects correctly on microphysical processes. The key quantities that ultimately determine the latent-heat release and its vertical distribution in the GCM grid-box are the grid-mean evaporation and precipitation rate. These quantities are shown for the three precipitation schemes in Fig. 4. Figure 4(a) shows the vertical distribution of evaporation rate. As for precipitation fraction the agreement between the JK99 model and the new parametrization is excellent from the model top to model level 20, whereas the T93 scheme overestimates evaporation in model levels 16 and below. The main reasons for this overestimation have been identified by JK99 as the overestimation of precipitation fraction (see Fig. 3) and the use of a single (grid-mean) flux in all microphysics calculations. The new parametrization, although distinguishing between clear-sky and cloudy precipitation flux, still averages at the bottom of each level within these two categories. This, as a consequence of the vertical distribution of cloud fraction (Fig. 2), leads to the strong overestimation of evaporation evident in Fig. 4(a) in model level 20. A large cloudy precipitation flux builds up in the very small fraction which is cloudy from cloud top (model level 5) to the base of level 18. In model level 19, this large flux is (wrongly) spread out (averaged) over the larger cloud fraction in that level. Due to a reduction in cloud fraction in the next level below (model level 20) this large flux is partly made available for evaporation in that level. In the more accurate JK99 subgrid model this 'spreading out' does not

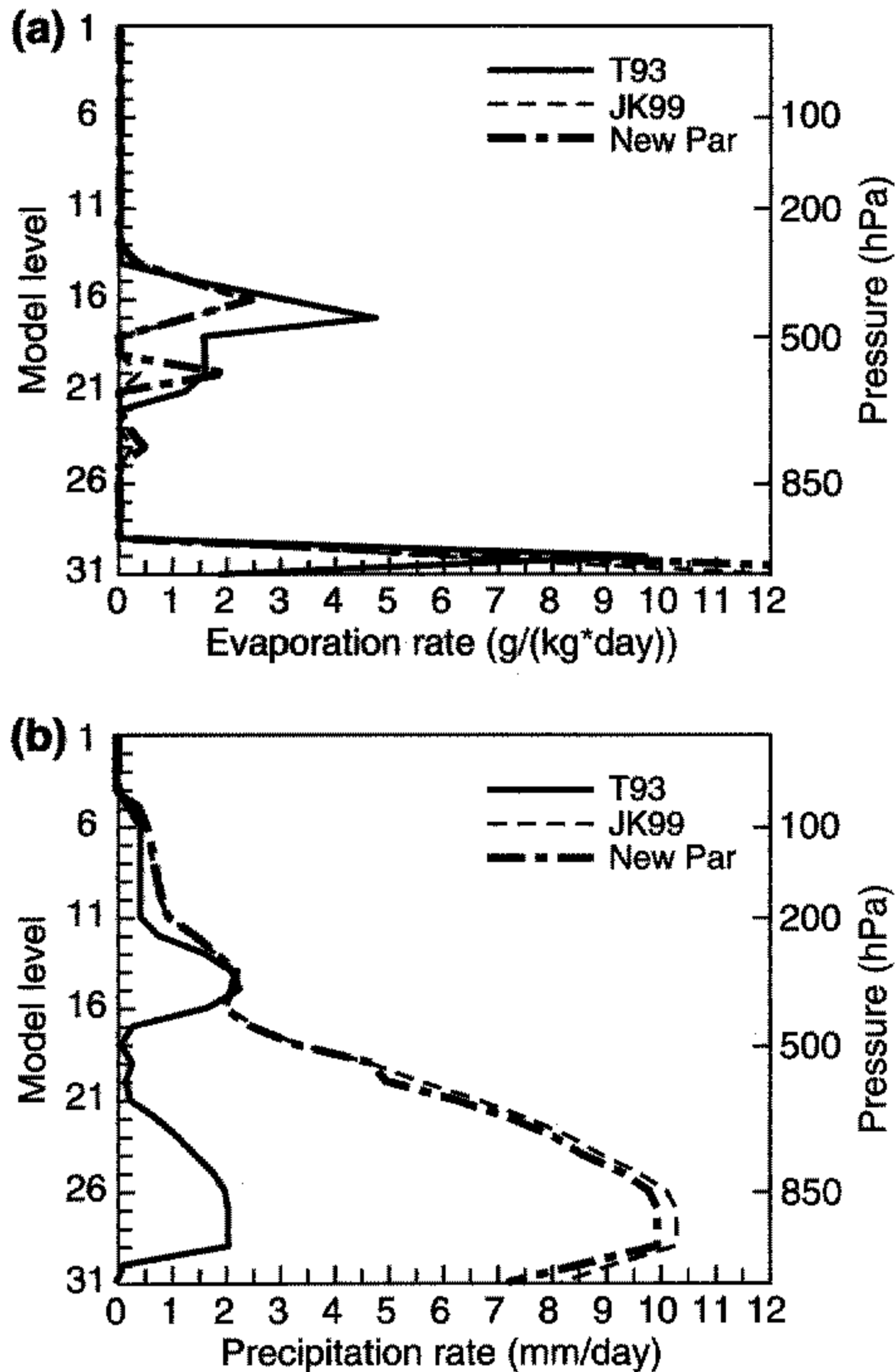


Figure 4. Grid-mean (a) evaporation rate and (b) precipitation rate as predicted in a single time step by the T93 parametrization, the JK99 subgrid model, and the new parametrization (New Par). See text for further explanation.

occur, so that here only the precipitation generated in model level 19 itself is available for evaporation, leading to much smaller evaporation rates. Also note that the overestimation of precipitation evaporation in levels 23 and 24 results from the same error in parametrization.

The effect of the overestimated evaporation is also seen in the grid-mean precipitation flux (Fig. 4(b)), for which the new parametrization agrees extremely well with the JK99 model down to level 20. Below that the precipitation flux is underestimated. The differences are, however, considerably smaller than between the T93 parametrization and the JK99 model.

Despite the obvious limitations of the new parametrization as outlined above, the major shortcomings of the T93 scheme for the single-column case are largely alleviated.

(b) Global model

Although the single-column-model results give an indication on how a parametrization change affects the model results, the cases chosen may have a limited representativeness. It is therefore necessary to assess the performance of the schemes in the full global model. Figures 5 and 6 show the zonal mean distribution of precipitation fraction and evaporation rate as predicted by the three schemes for the first time step of a T63L31 version of the ECMWF global model.

The largest difference in the prediction of precipitation fraction between the T93 (Fig. 5(a)) and the JK99 (Fig. 5(b)) models occurs in the tropics. Here the T93 scheme shows a monotonic increase in precipitation fraction from the cloud top to the surface. The reasons for this increase are discussed in JK99. In contrast, the new parametrization (Fig. 5(c)) represents the 'true' distribution of precipitation fraction as given by the JK99 model very well. There is a slight overestimation of precipitation fraction (about 10%) in the upper tropical troposphere. This is most probably caused by averaging problems similar to those described earlier, but in clear sky. The clear-sky precipitation in the JK99 model is not homogeneously distributed in the horizontal due to cloud-cover variations in the upper troposphere (see Fig. 2). Hence, in some parts of the clear-sky fraction, sublimation will reduce the precipitation flux to zero earlier than in others. This effect cannot be captured by a single clear-sky flux as used here, since the averaging within clear sky will implicitly transport precipitation from regions with large values to regions with small values, while keeping the precipitation fraction constant at too large a value.

As expected from the single-column results, the T93 scheme overestimates the evaporation of precipitation in the tropical mid-troposphere (by up to a factor of two in the zonal mean). The new parametrization constitutes a major improvement. There is, however, a residual overestimation of evaporation of precipitation, indicating that the single-column case and the problems therein are typical for the tropics.

In the extratropics the new parametrization improves the representation of precipitation fraction. However, there are only small effects on evaporation, which is already in good agreement with the T93 scheme. JK99 speculate that this better agreement is due to much smaller vertical variations in cloud cover in these regions, and hence a smaller influence of the new parametrization.

Finally, Figure 7 presents the zonal mean distribution of large-scale precipitation (i.e. precipitation produced by the schemes discussed here). As expected from the previous Figures the T93 scheme strongly underestimates precipitation at the surface in the tropics. This major problem of the T93 scheme is removed when applying the new precipitation scheme.

In summary, the new parametrization, although still exhibiting some easily understandable problems, captures the main effects of the vertical variation of cloud fraction on the parametrized precipitation fluxes as identified in the JK99 approach.

4. THE INFLUENCE OF THE NEW PARAMETRIZATION ON THE MODEL CLIMATE

The previous section demonstrated that the new parametrization significantly alters the behaviour of the large-scale precipitation generation and dissipation terms of the ECMWF model. In this section the influence of those changes on the model climate will be investigated. For that purpose the model was integrated for 4 months at spectral resolution T63 using 31 model levels in the vertical. The initial dates chosen were 26 April 1987, 1 May 1987, 5 May 1987, 27 October 1987, 1 November 1987, and 6 November 1987. Initial conditions were taken from ECMWF re-analysis fields. The sea surface temperatures were prescribed. The spring initial dates were used to create

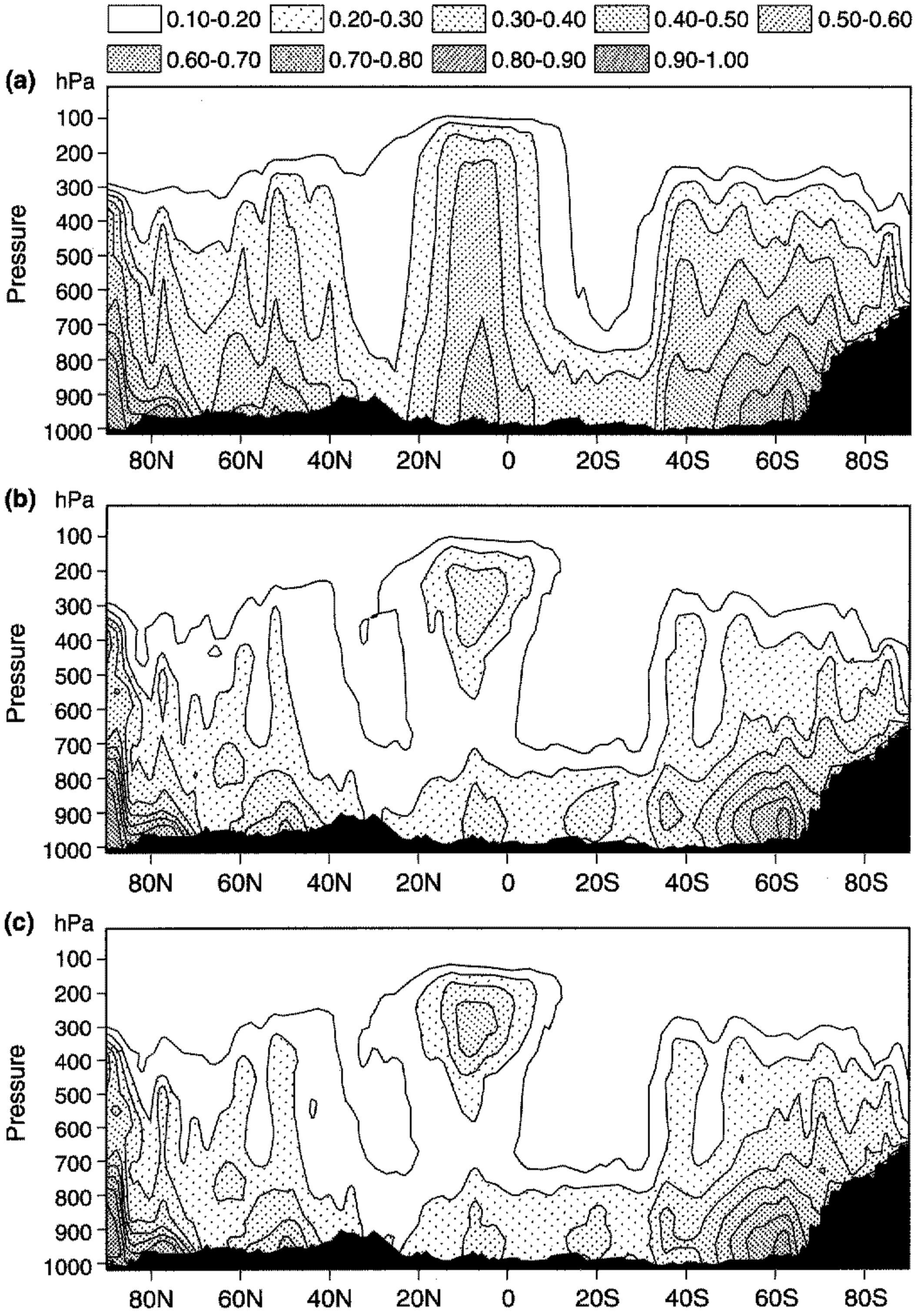


Figure 5. Precipitation fraction as predicted in a single time step by (a) the T93 parametrization, (b) the JK99 subgrid model, and (c) the new parametrization. See text for further explanation.

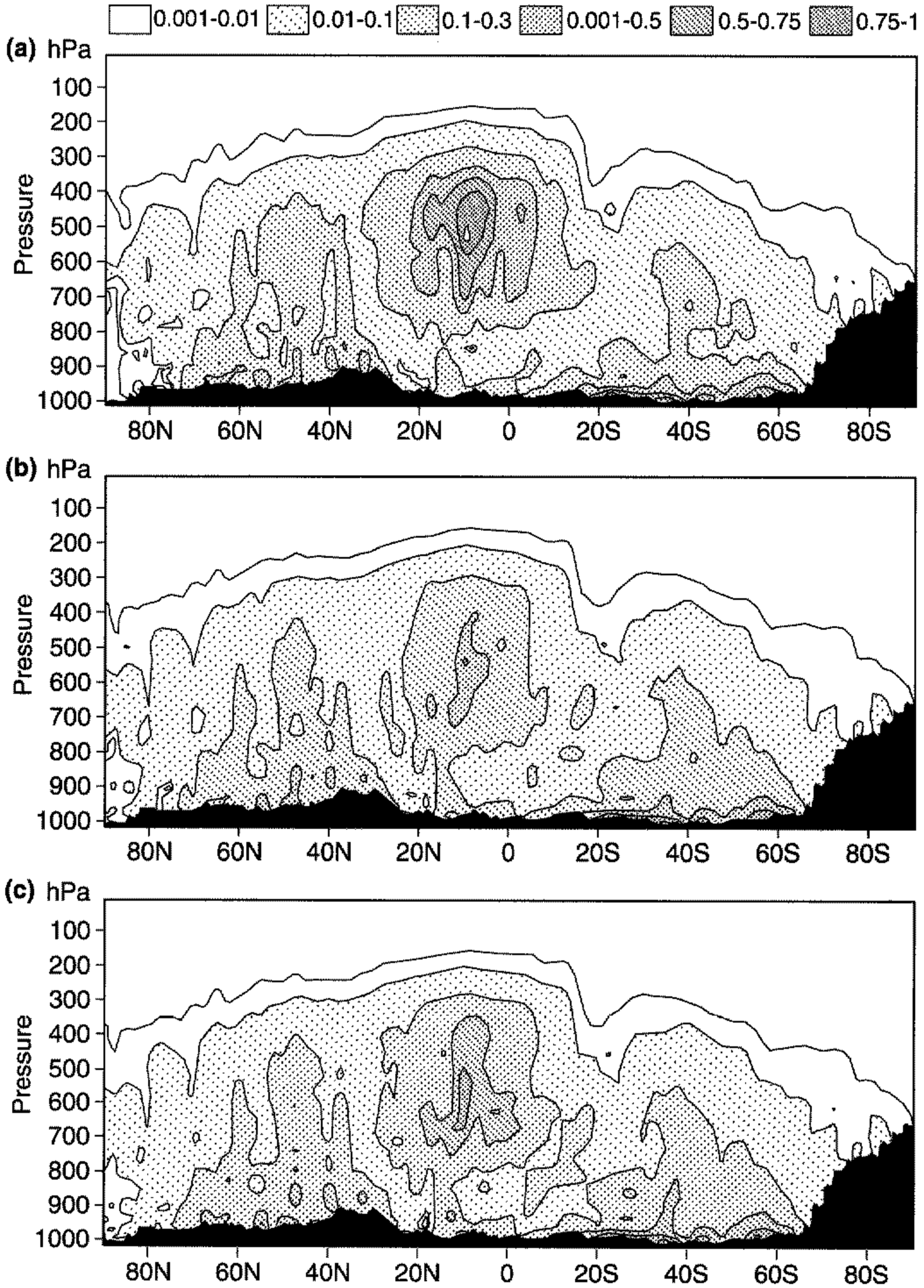


Figure 6. Evaporation rate (g (kg day)^{-1}) as predicted in a single time step by (a) the T93 parametrization, (b) the JK99 subgrid model, and (c) the new parametrization. See text for further explanation.

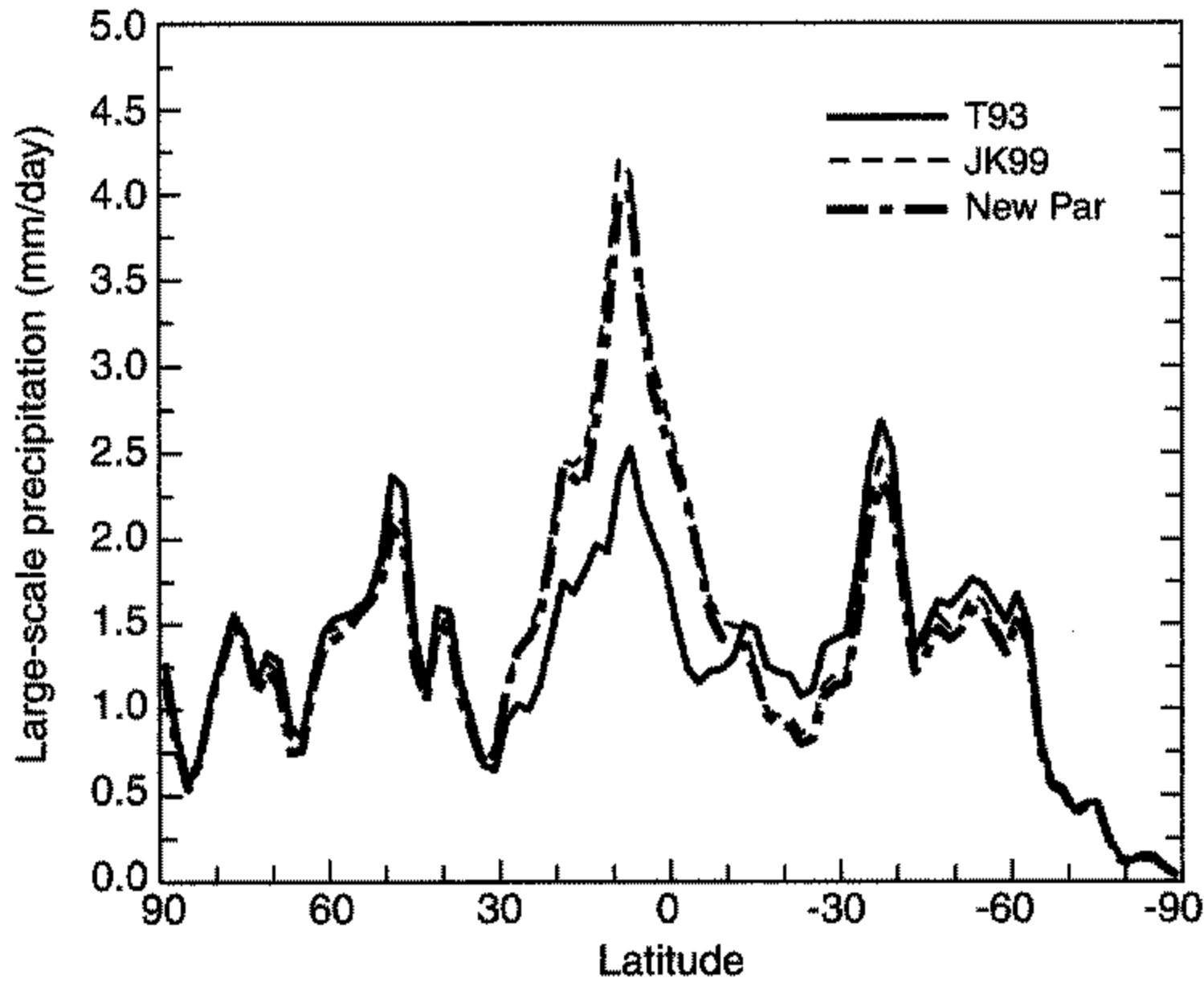


Figure 7. Zonal mean large-scale precipitation as predicted in a single time step by the T93 parametrization, the JK99 subgrid model, and the new parametrization (New Par). See text for further explanation.

ensemble average results for June–July–August 1987 (JJA87) and the autumn initial dates for average results for December–January–February 1987/88 (DJF87/88). The six integrations were carried out for both the current parametrization (Control) and the scheme described above (New Par). For detailed studies of individual components of the model's hydrological cycle, shorter (30-day) integrations were carried out for both parametrizations using re-analysis data for 1 July 1998 as an initial condition.

One of the parameters that exhibited large differences between the schemes in the first time step was the large-scale precipitation at the surface (Fig. 7). Figure 8 shows the same quantity for the ensemble average of the three JJA87 integrations. The sign of the differences, with the new scheme predicting more precipitation in the tropics and less in most of the extratropical latitudes, is the same as in the initial time step. The magnitude, however, is greatly reduced. The maximum difference in the tropics is now of the order of 8% as compared with 60% in the first time step. This indicates an adjustment process that offsets the direct effect of the new parametrization to evaporate less precipitation in the tropical mid-troposphere (see Fig. 6).

A possible process contributing to the model adjustment is a drying of the tropical mid-troposphere due to the reduced evaporation of precipitation. This constitutes a negative feedback since more precipitation can evaporate in a drier environment. Figure 9 provides evidence for the occurrence of this feedback in the model. In both seasons the relative humidity of the mid-troposphere is reduced by about 4 to 6%, with the larger reduction in winter. Changes in the zonal mean temperature field, however, are much less noticeable, being less than 0.2 K everywhere within the tropics (not shown).

Figure 10 provides a detailed schematic of the model's water reservoirs and conversion rates averaged over 30 days of a T63L31 integration in the tropics (20°N to 20°S), and shows the values for the integration using the new parametrization, with those for the control model shown in parentheses. Several interesting details emerge. The increase in large-scale precipitation of about 0.1 mm day⁻¹ that was already evident in Fig. 8 is

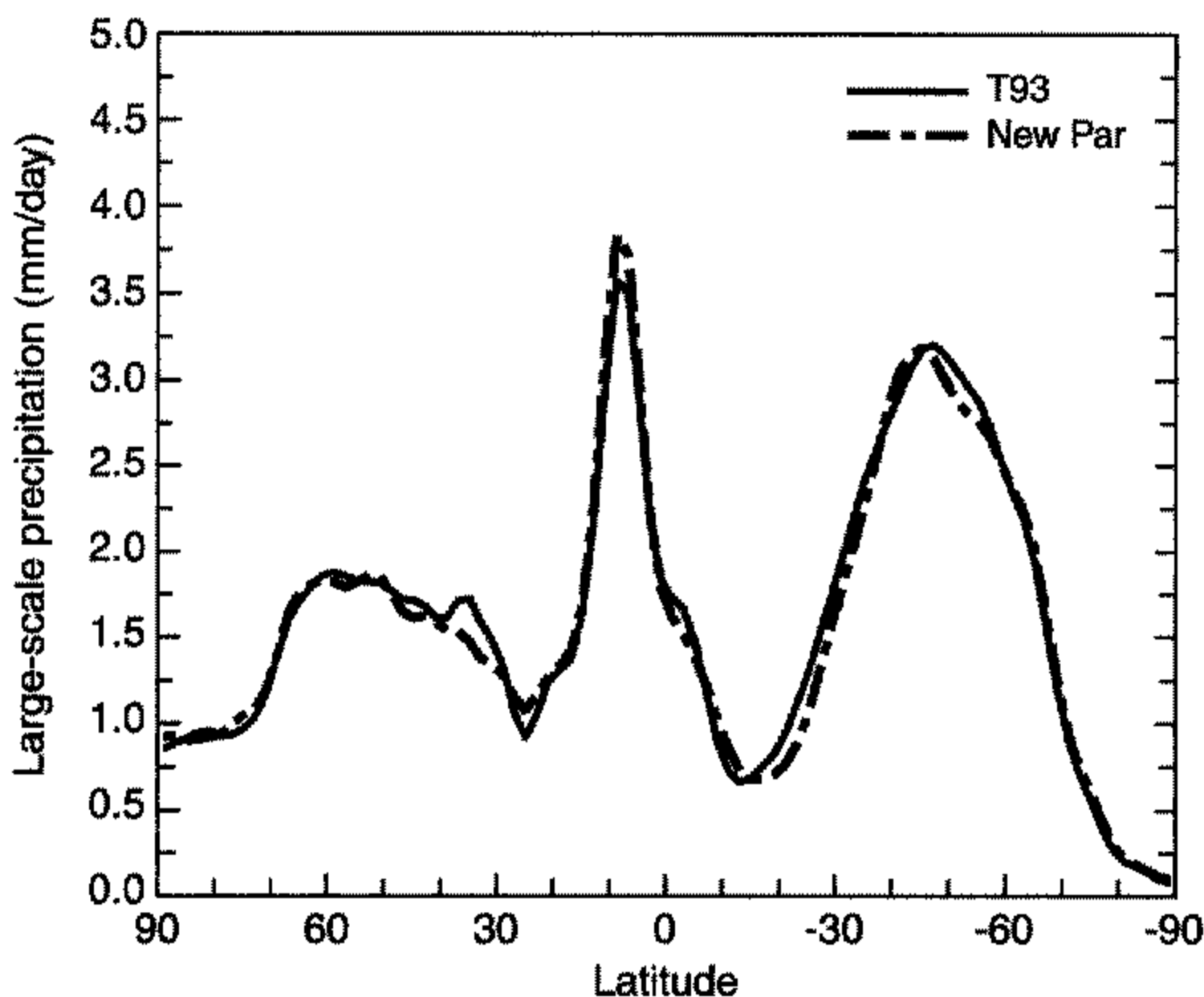


Figure 8. Zonal mean large-scale precipitation for June–July–August 1987 from an ensemble of three integrations using the T93 and new (New Par) precipitation schemes. See text for further explanation.

mainly due to a reduction in the evaporation of precipitation which is of the same order. The cloud liquid-water/ice content has been reduced by slightly more than 10%. Despite this, the conversion to precipitation has not changed much in magnitude, indicating a higher efficiency in that process, e.g. through higher accretion rates in the cloudy fluxes. The drying of the mid-troposphere is apparent in the vertically integrated water vapour (q), which is reduced by 1 kg m^{-2} (i.e. mm water). The convective activity, as measured by the condensation in cumulus updraughts, has slightly decreased, possibly due to entrainment of drier mid-tropospheric air into the convective updraughts. This leads to a slight decrease in the convective source of cloud liquid-water/ice, with the convective precipitation largely unaltered.

Figure 11 shows the time evolution over the first ten forecast days of the differences in some of the terms shown in Fig. 10 between the new parametrization and the control model. Here day 0 represents the first model time step. In the first time step the new parametrization produces significantly more large-scale precipitation due to (i) a decrease in evaporation, and (ii) an increase in the conversion to rain. The former has been extensively described in previous sections. The latter is due to the fact that the separate accounting of clear and cloudy precipitation fluxes in the new parametrization eliminates the 'horizontal' transport of precipitation from cloud to clear sky which occurs in the original parametrization through averaging effects. Consequently, the new parametrization yields higher in-cloud precipitation rates, and as a result warm-phase accretion increases significantly. No accretion is assumed to occur in the pure ice phase (temperature $< -23^\circ\text{C}$), hence there is no increase in the generation of snow. A fairly fast adjustment (1 to 3 days) occurs in the precipitation-conversion terms together with the reduction in cloud liquid-water/ice described above. After day 3, apart from variations in the cloud liquid-water/ice differences around a lower mean, the only significant changes occur in the differences of large-scale precipitation and evaporation. This is due to the much slower process of drying the tropical mid-troposphere (not

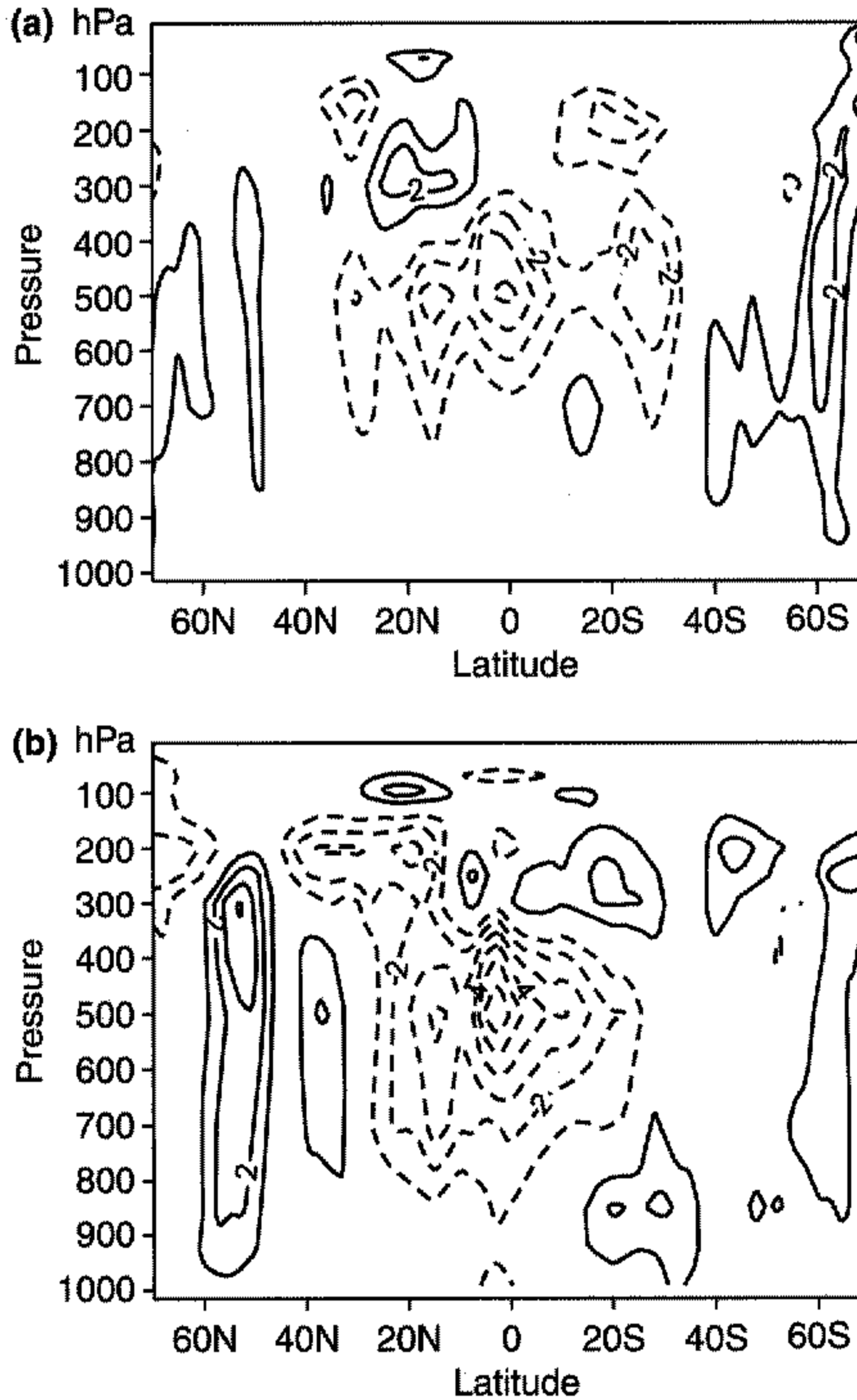


Figure 9. Zonal mean cross-section of relative humidity difference (new minus current) for ensembles of three integrations for (a) June–July–August 1987 and (b) December–January–February 1987/88. Contours are every 1% and negative values are shown dashed.

shown) which occurs on the typical humidity time-scale of the tropics of about 10 days. At day 10 both large-scale precipitation and evaporation difference have almost reached their 30-day average value (see Fig. 10).

5. DISCUSSION

It has been shown that the new parametrization of cloud and precipitation overlap introduced in section 2 provides a better description of the effects of this overlap on the microphysical processes. It is shown that, as a result of this, individual components of the hydrological cycle of the ECMWF global atmospheric model are significantly altered. The model climate is affected to a moderate extent. An obvious outstanding question in this investigation is whether the resulting changes constitute an improvement when compared with observations. There are two major caveats when attempting

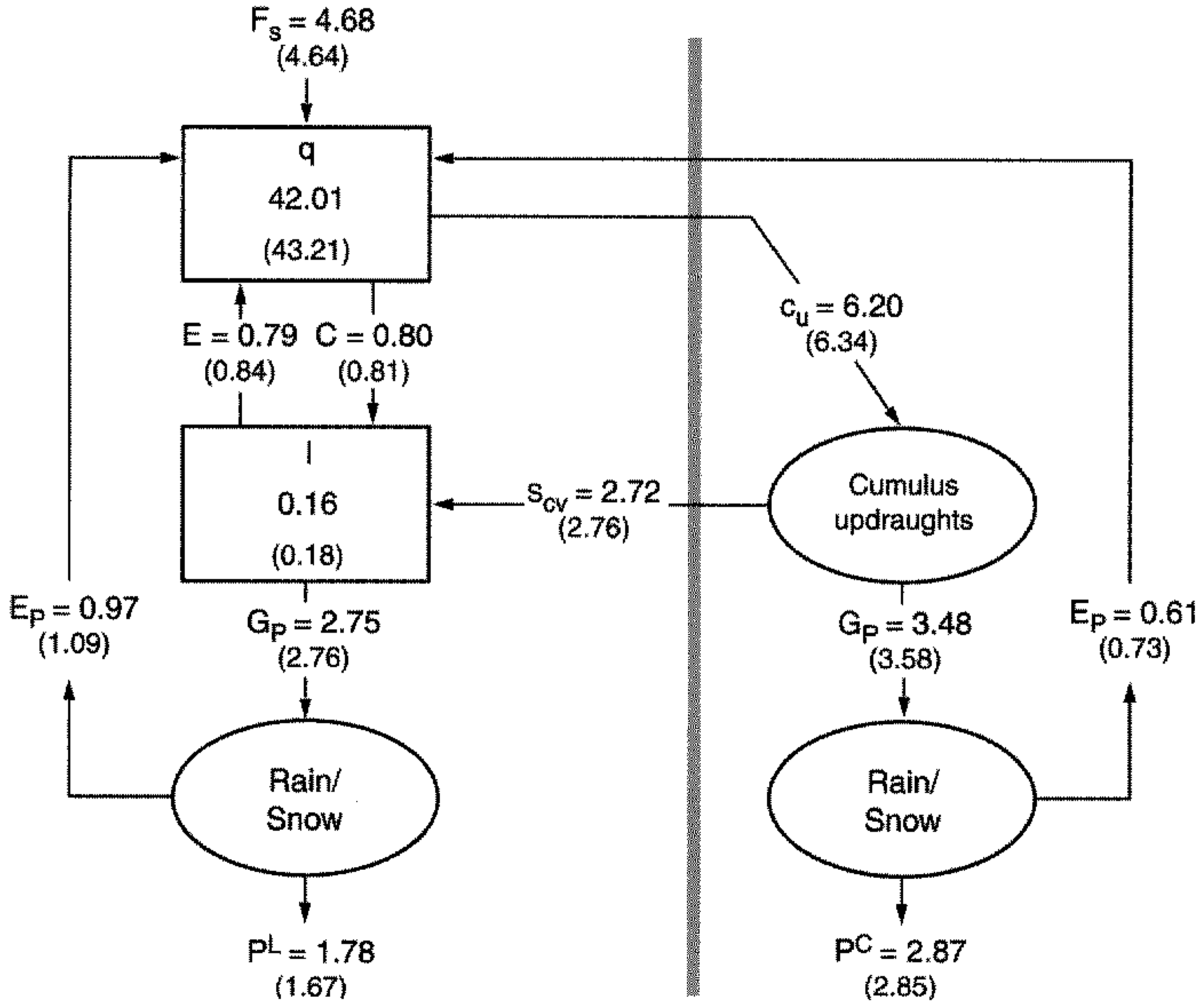


Figure 10. Hydrological cycle: tropical average (20°N to 20°S) of atmospheric water vapour q , cloud liquid-water/ice content l , and conversions between water vapour, cloud water/ice and rain/snow, in stratiform clouds (left) and cumulus updraughts (right). The results are averages over a 30-day integration at T63L31 initialized on 1 July 1998 with the new scheme, with values for the control model shown in parentheses. Units are mm for water reservoirs and mm day⁻¹ for conversion terms. The terms are: F_s —surface evaporation, C —large-scale condensation of cloud liquid/ice, E —large-scale evaporation of cloud liquid-water/ice, S_{CV} —source of cloud liquid water/ice from convection, G_P —generation of precipitation, E_P —evaporation of precipitation, c_u —condensation in cumulus updraughts, P^L —large-scale precipitation at the surface, and P^C —convective precipitation at the surface.

to answer this question. First, the parameters that show the largest sensitivity, such as mid-tropospheric tropical humidity, stratiform precipitation fraction, and evaporation rate, are either difficult or, as in the case of evaporation rate, impossible to measure directly, in particular on a global scale. Second, although it has been proven that the new parametrization captures overlap effects much better than the current one (see section 3) there is no reason that this alone should automatically lead to improved model results. This is due to uncertainties in other parts of the parametrization, most prominently perhaps the formulation of the microphysical parametrization itself. In the case of T93 for instance, artificial thresholds for relative humidity have been set above which evaporation of precipitation is suppressed. The values range from 70% in convective situations to 80% elsewhere. These low threshold values in the control model have compensated for the overprediction of evaporation which results from the insufficiently accurate description of overlap effects in T93. However, in order to study the impact of the new parametrization directly these threshold values were retained in the simulations with

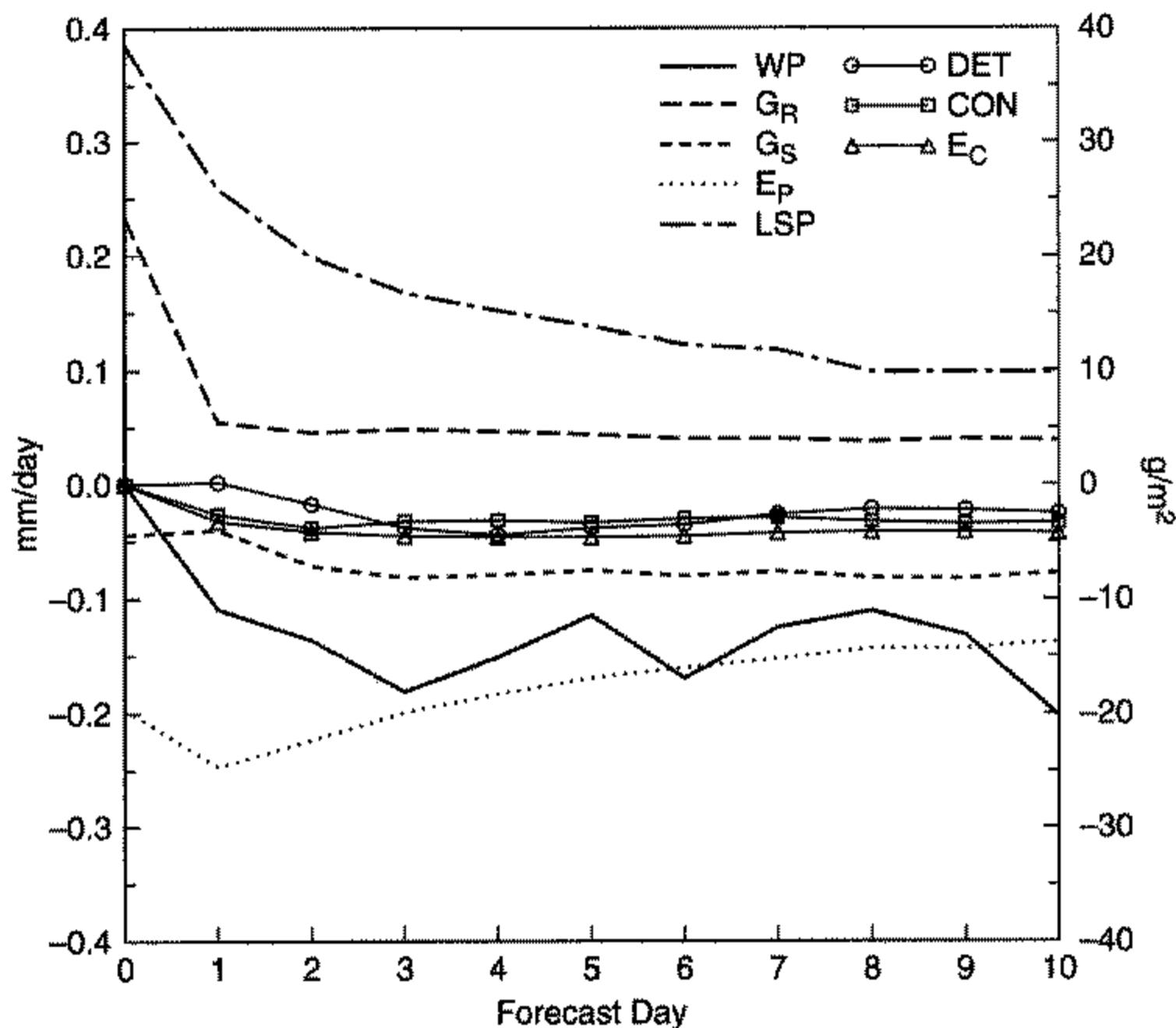


Figure 11. Hydrological cycle: time series of the difference (New Par – T93) (see text) in the tropical average (20°N to 20°S) of some terms shown in Fig. 10 for the first ten forecast days. Day 0 represents the first model time step. The terms are: WP—liquid+ice water path, G_R —generation of rain, G_S —generation of snow, E_P —evaporation of large-scale precipitation, LSP—large-scale precipitation at the surface, DET—source of cloud liquid-water/ice from convective detrainment, CON—large-scale condensation of cloud liquid water/ice, and E_C —large-scale evaporation of cloud liquid-water/ice.

the new parametrization presented in this paper. Assessing the impact of changing the thresholds is beyond the scope of the work presented here. Another major uncertainty lies in the choice of the cloud-overlap assumption actually used in the scheme. JK99 investigated the effects this choice can have in single time-step experiments (see Fig. 16 in JK99). The differences they found in precipitation for different overlap assumptions are of the same order as those brought about by the introduction of the new parametrization (Fig. 7). There is very little guidance from observations as to which overlap assumption is most realistic. The use of the maximum-random assumption here is broadly consistent with cloud-overlap statistics provided by Tian and Curry (1989). Recently available data on cloud vertical structure collected from cloud radar observations should provide some more guidance on this issue in the near future.

A very important parameter of the new parametrization is the fractional coverage of precipitation in a grid-box. This parameter determines the local values of the precipitation flux and hence the ‘intensity’ with which various microphysical processes can act. Furthermore it is a parameter that is in principle measurable for instance by using a scanning precipitation radar. One such set of measurements has been published by Sui *et al.* (1997) for an extended period of ship-borne radar measurements with a scan range of 150 km during TOGA-COARE*. In order to assess the performance of both the T93 and the new parametrization in simulating precipitation fraction a 30-day integration at T63L31 (about 200 km horizontal resolution) for December 1992 has been carried out. Figure 12 shows the precipitation fraction derived from the observations, and from

* The Coupled Ocean–Atmosphere Response Experiment of the Tropical Ocean and Global Atmosphere programme.

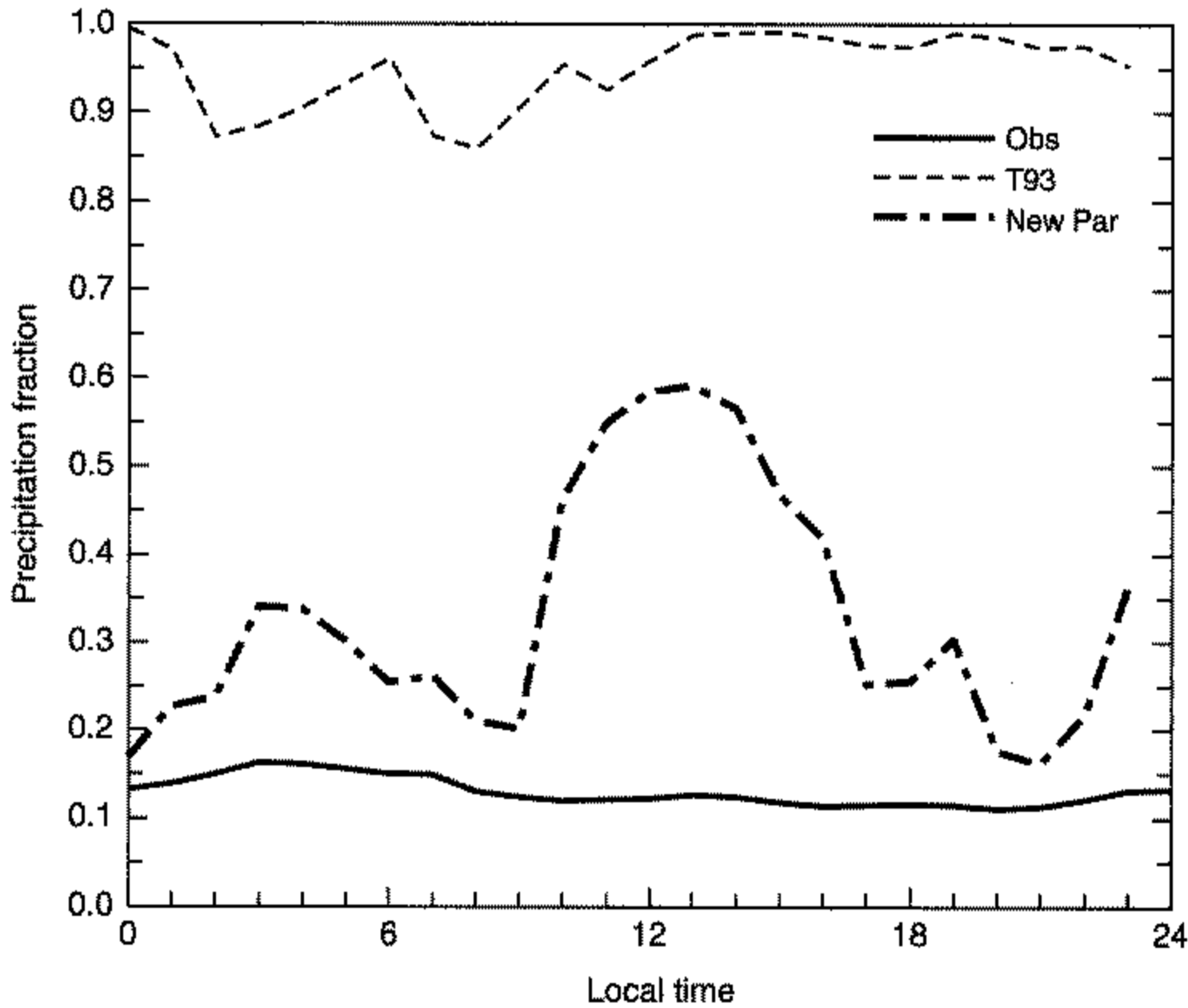


Figure 12. Monthly average stratiform (i.e. large-scale) precipitation fraction at the surface as a function of local time. Shown are observations by ship-borne radar during TOGA-COARE (Obs) and predictions for December 1992 at 2°S and 155°E by a T63L31 integration using the T93 scheme (T93) and the new parametrization (New Par). See text for further explanation.

the two model integrations at a grid point located at 2°S and 155°E , as a function of local time of day. Note that because of the 'climate' nature of the model integration the comparison can only be qualitative and should be interpreted in that way. The observed values are typically between 0.1 and 0.15, whereas the T93 parametrization predicts values that are always larger than 0.85. The new parametrization yields values of 0.2 to 0.6 with an unrealistically large diurnal maximum around local noon. This is very likely due to sampling problems since averaging the model results over a larger area removes the peak (not shown). Although still higher than observed, the results of the new parametrization constitute a major improvement. It should again be emphasized that this comparison is only meant to highlight the possibility of comparing some of the crucial parameters of the new parametrization scheme with observations.

One of the biggest advantages of the new scheme is that it improves the knowledge about which microphysical parametrization to apply over which part of the grid-box, and that it produces better estimates of the local precipitation rates needed in those parametrizations. A proper treatment of cloud and precipitation overlap along the lines presented in this study can therefore be seen as a prerequisite for the successful application in GCMs of complex microphysical schemes, as they are applied in cloud resolving and/or mesoscale models.

6. CONCLUSIONS

A new parametrization for cloud and precipitation overlap for use in GCMs has been developed. It is based on distinguishing cloudy and clear-sky precipitation fluxes during the descent of the precipitation through the model layers. The scheme has been introduced into the ECMWF global forecast model. Extensive single time-step tests against a subgrid precipitation model developed by Jakob and Klein (1999) show the

superiority of the new scheme over the current parametrization. The main change in the model physics is a reduction of precipitation evaporation in the tropical mid-troposphere and an increase in the conversion of cloud water to rain due to enhanced accretion. The scheme has a moderate effect on the model climate through a decrease of the tropical mid-tropospheric relative humidity by 4 to 8% depending on season. The tropical large-scale precipitation is increased by about 8%. By design, the new parametrization produces better estimates of local precipitation fluxes involved in the microphysical processes and therefore paves the way for increased complexity in their parametrization.

ACKNOWLEDGEMENTS

The authors would like to thank Drs A. Beljaars, L. Donner, M. Koehler and M. Miller for their comments on an early version of the manuscript. We are grateful for the comments of two anonymous reviewers which led to a further improvement of the text. C. H. Sui is acknowledged for providing the TOGA-COARE radar data. We would also like to thank Rob Hine for his help in preparing some of the figures.

REFERENCES

- | | | |
|--|------|---|
| Bechthold, P., Pinty, J. P. and Mascart, P. | 1993 | The use of partial cloudiness in a warm-rain parameterization: A subgrid-scale precipitation scheme. <i>Mon. Weather Rev.</i> , 121 , 3301–3311 |
| Fowler, L. D., Randall, D. A. and Rutledge, S. A. | 1996 | Liquid and ice cloud microphysics in the CSU general circulation model. Part I: Model description and simulated microphysical processes. <i>J. Climate</i> , 9 , 489–529 |
| Ghan, S. J. and Easter, R. C. | 1992 | Computationally efficient approximations to stratiform cloud microphysics parameterization. <i>Mon. Weather Rev.</i> , 120 , 1572–1582 |
| Heymsfield, A. J. and Donner, L. J. | 1990 | A scheme for parameterizing ice-cloud water content in general circulation models. <i>J. Atmos. Sci.</i> , 47 , 1865–1877 |
| Jakob, C. and Klein, S. A. | 1999 | The role of vertically varying cloud fraction in the parametrization of microphysical processes in the ECMWF model. <i>Q. J. R. Meteorol. Soc.</i> , 125 , 941–965 |
| Lohmann, U. and Roeckner, E. | 1996 | Design and performance of a new cloud microphysics scheme developed for the ECHAM general circulation model. <i>Clim. Dyn.</i> , 12 , 557–572 |
| Manabe, S., Smagorinsky, J. and Strickler, R. F. | 1965 | Simulated climatology of a general circulation model with a hydrological cycle. <i>Mon. Weather Rev.</i> , 93 , 769–798 |
| Rasch, P. J. and Kristjansson, J. E. | 1998 | A comparison of the CCM3 model climate using diagnosed and predicted condensate parameterizations. <i>J. Climate</i> , 11 , 1587–1614 |
| Rotstayn, L. D. | 1997 | A physically based scheme for the treatment of stratiform clouds and precipitation in large-scale models. I: Description and evaluation of the microphysical processes. <i>Q. J. R. Meteorol. Soc.</i> , 123 , 1227–1292 |
| Slingo, J. M. | 1987 | The development and verification of a cloud prediction scheme for the ECMWF model. <i>Q. J. R. Meteorol. Soc.</i> , 113 , 899–927 |
| Smith, R. N. B. | 1990 | A scheme for predicting layer clouds and their water content in a general circulation model. <i>Q. J. R. Meteorol. Soc.</i> , 116 , 435–460 |
| Sui, C.-H., Lau, K.-M., Takayabu, Y. N. and Short, D. A. | 1997 | Diurnal variations in tropical ocean cumulus convection during TOGA COARE. <i>J. Atmos. Sci.</i> , 54 , 639–655 |
| Sundqvist, H. | 1988 | 'Parameterization of condensation and associated clouds in models for weather prediction and general circulation simulation'. Pp. 433–461 in <i>Physically-based modelling and simulation of climate and climate change</i> . Ed. M. E. Schlesinger. Kluwer |
| Tian, L. and Curry, J. A. | 1989 | Cloud overlap statistics. <i>J. Geophys. Res.</i> , 94 , 9925–9935 |
| Tiedtke, M. | 1993 | Representation of clouds in large-scale models. <i>Mon. Weather Rev.</i> , 121 , 3040–3061 |